Atmos. Chem. Phys. Discuss., 7, 429–468, 2007
www.atmos-chem-phys-discuss.net/7/429/2007/

Atmospheric Chemistry and Physics Discussions

SCIAMACHY tropospheric NO_2 over the Alpine region and importance of pixel surface pressure for the column retrieval

D. Schaub[1], K. F. Boersma[2], J. Keller[3], D. Folini[1], D. Brunner[1], B. Buchmann[1], H. Berresheim[4], and J. Staehelin[5]

[1]Empa, Swiss Federal Laboratories for Materials Testing and Research, Ueberlandstrasse 129, CH-8600 Duebendorf, Switzerland
[2]Division of Engineering and Applied Sciences, Harvard University, Cambridge, Massachusetts, USA
[3]Paul Scherrer Institute (PSI), CH-5232 Villigen PSI, Switzerland
[4]German National Meteorological Service, DWD/MOHp, 82383 Hohenpeissenberg, Germany
[5]Swiss Federal Institute of Technology (ETH), Universitätstrasse 16, CH-8092 Zurich, Switzerland

Received: 23 November 2006 – Accepted: 8 January 2007 – Published: 12 January 2007

Correspondence to: D. Brunner (dominik.brunner@empa.ch)

Abstract

This study evaluates NO_2 vertical tropospheric column densities (VTCs) retrieved from measurements of the Scanning Imaging Absorption Spectrometer for Atmospheric Chartography (SCIAMACHY) above Switzerland and the Alpine region. A clear relationship between a spatially and temporally highly resolved Swiss NO_x emission inventory and SCIAMACHY NO_2 columns under anticyclonic meteorological conditions supports the general ability of SCIAMACHY to detect sources of NO_x pollution in Switzerland. Summertime NO_x lifetime estimates derived from this relation agree reasonably with values from literature. A further evaluation of the SCIAMACHY data is based on the comparison with NO_2 VTCs retrieved from the Global Ozone Monitoring Experiment (GOME). The annual mean NO_2 VTCs calculated from both data sets clearly show the advantage of the improved SCIAMACHY pixel resolution for qualitatively estimating the NO_x pollution distribution in a small country such as Switzerland. However, a more quantitative comparison of seasonally averaged NO_2 VTCs gives evidence for SCIAMACHY NO_2 VTCs being systematically underestimated over the Swiss Plateau during winter. A possible explanation for this problem (not reported in earlier literature) is the use of inaccurate satellite pixel surface pressures derived from coarsely resolved global models in the retrieval. The marked topography in the Alpine region can lead to deviations of several hundred meters between the assumed and the real mean surface height over a pixel. A sensitivity study based on selected clear sky SCIAMACHY NO_2 VTCs over the Swiss Plateau and two fixed a priori NO_2 profile shapes indicates that inaccurate pixel surface pressures have a considerable effect of up to 40% on the retrieved NO_2 columns. For retrievals in the UV-visible spectral range with a decreasing sensitivity towards the earth's surface, this effect is of major importance when the NO_2 resides close to the ground, which occurs most pronounced during the winter season.

ACPD

7, 429–468, 2007

1 Introduction

Nitrogen dioxide is an important air pollutant. It can affect human health and plays a major role in the production of tropospheric ozone (Seinfeld and Pandis, 1998; Finlayson-Pitts and Pitts, 2000). The bulk of NO_x is emitted by the high-temperature combustion of fossil fuel in the highly industrialised continental regions in the northern mid-latitudes. Important natural sources are biomass burning and the microbial production in soils of the non-polar continental surface. At higher altitudes in the troposphere NO_x is directly injected into the troposphere by lightning and aircraft emissions (IPCC, 2001).

NO_x is primarily emitted as NO which oxidises to NO_2within a few minutes. The NO_2 concentration is affected by the partitioning of NO_x into NO and NO_2 which depends on the abundance of ozone and reactive organic compounds as well as on solar light intensity and temperature, and which therefore changes with altitude and with time of day in the troposphere. NO_x is removed from the troposphere mainly by conversion to nitric acid (HNO_3). During daytime, HNO_3 is formed through the reaction of NO_2 with the OH radical. At night, a two step reaction mechanism forms nitrogen pentoxide (N_2O_5) which further reacts on surfaces and aerosol to HNO_3 (Dentener and Crutzen, 1993). HNO_3 is finally removed by dry and wet deposition (Kramm et al., 1995). The resulting NO_x lifetime is highly variable with an annual average boundary layer lifetime of about one day (Warneck, 2000). However, due to the higher summertime abundance of OH, much shorter lifetimes of a few hours prevail during photochemically active summer days. In this study, we infer NO_x lifetimes from the combination of SCIAMACHY NO_2 VTCs with a high-quality NO_x emission inventory to check the reliability of SCIAMACHY data. Generally, NO_x lifetimes are essential to determine emissions from space-borne data (e.g. Martin et al., 2003).

Although the NO_x ($\equiv$ NO + NO_2) concentration in Switzerland decreased during the last 15 years the Swiss NO_2 annual ambient air quality standard of 30 μgm^{-3} ($\approx$16 ppb) is still exceeded in polluted areas (FOEN, 2005). Monitoring of nitrogen oxides there-

ACPD
7, 429–468, 2007

EGU

fore plays an important role for the assessment of reduction measures. Complementary to ground-based monitoring networks which provide detailed information of local near-surface air pollution, space-borne instruments such as the Global Ozone Monitoring Experiment (GOME) (Burrows et al., 1999) and the Scanning Imaging Absorption Spectrometer for Atmospheric Chartography (SCIAMACHY) (Bovensmann et al., 1999) provide area-wide data of NO_2 vertical tropospheric column densities (VTCs) with global coverage within a few days. The improved resolution of space-borne NO_2 VTCs (GOME pixel size: $320\times40\,km^2$, SCIAMACHY: $60\times30\ km^2$, Ozone Monitoring Instrument (OMI): $13\times\ 24\,km^2$) increasingly allows to detect NO_2 pollution features on a regional scale. However, these space-borne data and their complex retrieval are emerging techniques and validation is needed. Schaub et al. (2006) summarised different validation campaigns of GOME and SCIAMACHY NO_2 data and carried out a detailed comparison of GOME NO_2 VTCs retrieved by KNMI (Royal Dutch Meteorological Institute) and BIRA/IASB (Belgian Institute for Space Aeronomy) with NO_2 profiles derived from ground-based in situ measurements at different altitudes in the Alpine region.

In this paper we evaluate SCIAMACHY NO_2 VTCs over Switzerland and the Alpine region with regard to their use for air quality monitoring and modelling on a regional scale. For the first time, the focus is on the size of a small country such as Switzerland. The above mentioned GOME validation approach presented in Schaub et al. (2006) can not be adopted for SCIAMACHY here. In that approach in situ measurements from a number of widely separated stations located at different altitudes in Switzerland and Southern Germany have been used to estimate vertical NO_2 columns. The size of SCIAMACHY pixels, however, is too small to justify the combination of measurements that are spatially separated (the latter are only used for a qualitative comparison in this study). We therefore first perform a qualitative evaluation by relating SCIAMACHY NO_2 VTCs to a spatially and temporally highly resolved NO_x emission inventory available for Switzerland, showing the general ability of SCIAMACHY data to detect the NO_2 pollution distribution on the scale of a small country. This comparison is then used to

infer seasonal mean daytime NO_x lifetimes that are subsequently compared to values from literature.

Further, the SCIAMACHY NO_2 VTCs are evaluated by a comparison with GOME NO_2 columns over Switzerland and a qualitative comparison with the seasonal variation of NO_2 columns deduced from ground-based in situ measurements carried out at different altitudes. Evidence is found for SCIAMACHY NO_2 VTCs being systematically underestimated over the Swiss Plateau during the winter season. We will present a plausible reason contributing to this problem which is related to an inadequate representation of the surface topography in the NO_2 retrieval. This problem potentially affects any region on the globe with a marked topography and becomes increasingly important with improving pixel resolution when the retrieval is based on coarsely resolved input parameters, e.g. derived from global models.

2 Data

2.1 KNMI/BIRA GOME and SCIAMACHY tropospheric NO_2 observations

Nadir measurements from GOME on board ESA's ERS-2 satellite and from SCIAMACHY on board ESA's Envisat satellite are used in the present study. The GOME and SCIAMACHY observations are obtained at approximately 10:30 and 10:00 local time and individual pixels cover an area of $320\times40\,km^2$ and $60\times30\,km^2$, respectively. The GOME and SCIAMACHY measurement principles are described in Burrows et al. (1999) and Bovensmann et al. (1999), respectively. The NO_2 VTCs studied in this work are the product of a collaboration between KNMI and BIRA/IASB. Both GOME and SCIAMACHY NO_2 data are publicly available on a day-by-day basis via ESA's TEMIS project (Tropospheric Emission Monitoring Internet Service, www.temis.nl).

The first retrieval step is based on the Differential Optical Absorption Spectroscopy (DOAS) technique (Vandaele et al., 2005): a modelled spectrum is fitted to the measured reflectance spectrum in the spectral window from 426.3–451.3 nm. The modelled

spectrum accounts for spectral absorption features of NO_2, O_3, O_2-O_2 and H_2O. Scattering by clouds, aerosols, air molecules and the surface is described by a low-order polynomial. This first retrieval step results in the slant column density (SCD) of NO_2, which can be interpreted as the column integral of absorbing NO_2 molecules along the effective photon path from the sun through the atmosphere to the spectrometer.

The second retrieval step separates the stratospheric contribution from the total SCD (Boersma et al., 2004). For KNMI retrievals this is achieved with a data-assimilation approach using the global TM4 chemistry transport model (CTM) (Dentener et al., 2003). The tropospheric SCD (SCD_{trop}) results from the subtraction of the stratospheric estimate from the total SCD.

In the third retrieval step, the SCD_{trop} is converted into a VTC by applying the tropospheric air mass factor (AMF_{trop}). Following Palmer et al. (2001) and Boersma et al. (2004), the retrieved SCIAMACHY NO_2 VTC (X_{SCIA}) is calculated as

$$X_{SCIA} = \frac{N_{trop}}{M_{trop}(\boldsymbol{x}_a, \boldsymbol{b})} = \frac{N_{trop} \cdot \sum_l x_{a,l}}{\sum_l m_l(\boldsymbol{b}) \cdot x_{a,l}} \quad (1)$$

where N_{trop} denotes the tropospheric slant column density, M_{trop} the tropospheric air mass factor, $x_{a,l}$ the layer specific subcolumns from the a priori profile $\boldsymbol{x}_a$, and m_l the altitude-dependent scattering weights. The latter are calculated with the Doubling Adding KNMI (DAK) radiative transfer model (Stammes, 2001) and best estimates for forward model parameters $\boldsymbol{b}$, describing surface albedo, cloud parameters (fraction, height) and pixel surface pressure. The a priori NO_2 profiles for every location and all times are obtained from the TM4 CTM. Cloud fraction and height are taken from the Fast Retrieval Scheme for Clouds from the Oxygen A band (FRESCO) algorithm (Koelemeijer et al., 2001). Since the TM4 model is driven by meteorological data of the European Centre for Medium-Range Weather Forecasts (ECMWF) the surface pressures in TM4 are taken from the ECMWF model on the $2^\circ \times 3^\circ$ resolution of the TM4 model. The surface pressure for an individual satellite pixel is linearly interpolated to the pixel location (hereafter ECMWF/TM4 surface pressure).

ACPD
7, 429–468, 2007

EGU

Errors of GOME tropospheric NO_2 retrievals have extensively been discussed in Boersma et al. (2004). Based on this work, errors for both GOME and SCIAMACHY NO_2 VTCs are estimated on a pixel-to-pixel basis and additionally provided in the TEMIS data sets. Error propagation studies have shown SCIAMACHY NO_2 VTC errors to be similar to GOME errors. However, these studies have not included the effect of surface pressure. The present work will show that, over a complex topography, this parameter can be expected to lead to larger errors for the higher resolved SCIAMACHY data.

2.2 Swiss NO_x emissions

Swiss NO_x emissions mount up to 33.2 kt N/year with traffic, industry, agriculture/forestry and residential activities contributing 58%, 24%, 12% and 6%, respectively, for the year 2000 (FOEN, 2005). The present study employs an hourly resolved NO_x emission inventory for Switzerland available on a $3\times3\,km^2$ grid. It combines the following basic data sets:

- Road traffic emissions of NO_x for the reference year 2000 with a spatial resolution of 250 m were prepared by the consulting company INFRAS, Switzerland. An average diurnal variation is provided as well. Long-term trends of annual totals recently published in Keller and Zbinden (2004) were used to interpolate the emissions between 2000 and 2005.
- NO_x emissions from residential activities, heating, industry, off-road traffic and agriculture/forestry for the reference year 2000 with a spatial resolution of 200 m and accounting for seasonal variations were prepared by the Meteotest company, Switzerland. Data sets for other years of interest were calculated on the basis of trends provided by the Swiss Federal Office for the Environment (FOEN, 1995).

Additional information on the emission inventory is summarised in Keller et al. (2005). Total emission inventories are usually based on a large number of input variables.

Each of these parameters – and, thus, also the resulting total emission inventory – are affected by uncertainties. Their assessment is a challenging task which needs further assumptions (e.g. Kühlwein and Friedrich, 2000). For the $3\times3\,km^2$ Swiss NO_x emission inventory an accuracy of ±15–20% is estimated in FOEN (1995). Kühlwein (2004) further pointed out increasing errors in emission inventories for increasing spatial resolutions. Thus, due to integration of the $3\times3\,km^2$ resolved emission data over the SCIAMACHY pixel size of $60\times30\,km^2$ in the present work, the above given error of 20% is considered as a reasonable upper limit, which will be assumed in this study.

3 Methods

3.1 Comparison of SCIAMACHY NO_2 VTCs with a high resolution emission inventory and estimation of mean NO_x lifetimes

SCIAMACHY NO_2 VTCs located entirely within the Swiss boundaries are related to the high resolution Swiss NO_x emission inventory presented in Sect. 2.2. NO_x emission rates between 9:00 and 10:00 (alternatively between 6:00 and 10:00) UTC are summed up over the individual pixel footprints.

First, the qualitative relation between NO_2 VTCs and collocated NO_x emissions is discussed (Sect. 4.1.1). Then, neglecting any transport into or out of the column enclosed by the satellite pixel, seasonal NO_x lifetimes are estimated simply as the ratio between the observed column (in N-equivalents: g(N) km^{-2}) and the emission rate (in g(N) $km^{-2}\,hr^{-1}$). In order to account for inaccuracies in both the observed columns and the emission rates, the lifetime estimates are based on the calculation of a weighted orthogonal regression (York, 1966). SCIAMACHY NO_2 VTC 1-sigma error estimates are taken from the TEMIS data file where error estimates are provided for each individual pixel (Boersma et al., 2004). For the NO_x emission rates added up over the individual SCIAMACHY pixels an error of 20% is assumed (Sect. 2.2).

SCIAMACHY NO_2 VTCs are converted to NO_x VTCs by employing representative

values for the seasonal mean NO_2/NO ratio. The latter depends on the abundance of ozone and reactive organic compounds as well as on solar light intensity and temperature. Thus, the ratio varies both spatially (horizontally and vertically) and seasonally. For the United States and based on 106 NO_x monitoring data sets measured at different distances from the predominant emission sources, Chu and Meyer (1991) recommended a national default value for the NO_2/NO ratio of 3. NO_x measurements operated since 1999 at a rural site at the edge of the Swiss Plateau (Rigi, 47° 04' N, 8° 28' E, 1030 m asl) using a standard chemiluminescence detector for the measurement of NO and a photolytic converter for the selective conversion of NO_2 to NO indicates a seasonal variation of monthly mean NO_2/NO ratios of between 1.6 (January) and 4.0 (August) for anticyclonic clear sky conditions and a time window between 10:00 and 12:00 UTC (Steinbacher, personal communication). Because the location of the measurement site on a mountain ridge roughly 500 m above the Swiss Plateau can lead to a decoupling from the near-ground Swiss Plateau air masses during winter and the NO_2/NO ratio is decreasing with height (e.g. Nakamura et al., 2003), we suppose that the wintertime ratio given above is rather low. Thus, for the present work, we assume seasonal mean NO_2/NO ratios of 3, 4, 3 and 2 for the spring (MAM), summer (JJA), fall (SON) and winter (DJF) season, respectively. Due to the bulk of NO_x residing near the ground in polluted regions we further assume these NO_2/NO ratios to be representative for the whole tropospheric column.

The NO_x emissions taking place at the location of the column are considered as the main flux of NO_x into the column which, in an equilibrium state, is balanced by the chemical and physical (i.e. deposition) losses in the column. Neglecting transport and assuming first order losses only and steady state, we can write

$$\frac{dM}{dt} = E - k \cdot M = 0 \quad (2)$$

and hence

$$M = \frac{1}{k} \cdot E = \tau \cdot E \quad (3)$$

with M the amount of NO_x in the column, E the NO_x emission rate (both converted to N-equivalents) and τ the lifetime. The basic assumption of steady state has also been made by Leue et al. (2001), Beirle et al. (2003) and Kunhikrishnan et al. (2004). It disregards the horizontal NO_x transport into and out of the column. This transport, however, leads to a smearing effect that is depending on the distribution of the NO_x emissions, the prevailing meteorology (e.g. wind speed and direction) and the chemical lifetime. For mapping isoprene emissions from space-borne data, Palmer et al. (2003) determined typical smearing length scales. For NO_x lifetimes in the order of hours to one day, this length scale is ~100 km (Martin et al., 2003). This might be problematic regarding the SCIAMACHY pixel size of $60\times30\,km^2$. However, anticyclonic clear sky conditions (which are the present focus) are known to be associated with low wind speeds, i.e. rather stagnant air, and fast photochemistry, which reduces the importance of horizontal transport in the boundary layer.

Significant transport over larger distances (e.g. from highly polluted regions in adjacent countries to Switzerland as described in Schaub et al. (2005) for a frontal passage) is considered to be unimportant for the anticyclonic days investigated here.

3.2 Sensitivity of SCIAMACHY NO_2 VTCs to varying pixel surface pressure

Following Sect. 2.1 the mean pixel surface pressure is one of the parameters used in the column retrieval. For both GOME and SCIAMACHY pixels with centre coordinates within the region of interest ROI_{CH} (Fig. 1) covering the whole Switzerland (6° E – 10.5° E, 45.75° N – 47.75° N) the deviations between the ECMWF/TM4 mean surface pressures used in the retrieval (p_{surf}) and the corresponding effective mean surface pressures (p_{eff}) are determined and compared to each other. p_{eff} over the pixel extension is determined from the aLMo (Alpine Model, the MeteoSwiss numerical weather prediction model) topography which better represents the real topography as the aLMo resolution of $7\times7\,km^2$ is much finer than the TM4 model grid (2°× 3°, $\sim220\times240\,km^2$).

An estimate of the effect of inaccurate pixel surface pressure used in the retrieval is carried out for a subset of clear sky SCIAMACHY pixels. The $AMFs_{trop}$ and NO_2 VTCs

are first calculated for p_{surf} as in the retrieval and then recalculated for the better surface pressure estimate p_{eff}. The criteria for the pixel subset are i) anticyclonic clear sky meteorological conditions (Alpine Weather Statistics; MeteoSwiss, 1985), ii) pixel cloud fraction ≤0.1, and iii) a small standard deviation <65 m of the aLMo 7°7 km^2 grid cell heights enclosed within a SCIAMACHY pixel, the latter ensuring that the reprocessing is done for pixels over a flat region in the vicinity of the Alps rather than over the complex Alpine topography. The resulting SCIAMACHY pixels are located above the north-eastern Swiss Plateau (Fig. 2).

The sensitivity test is based on two characteristic (and fixed) CTM a priori NO_2 profile shapes (Fig. 3). In a first profile (A), the bulk of the NO_2 is residing near the ground. Such profile shapes are expected to occur over polluted regions and most pronounced during the winter months when vertical mixing is generally weak or non-existing. A second profile (B) shows a much lower NO_2 abundance near the ground and can be expected to represent either a remote profile or a summertime profile shape resulting from vertical mixing. As shown in Fig. 3 the use of a different surface pressure scales the profile vertically. The other retrieval (or forward model) parameters including surface albedo, cloud fraction and height, solar zenith angle and so on are kept constant.

4 Results and discussion

4.1 SCIAMACHY NO_2 VTCs and NO_x emissions in Switzerland

4.1.1 Qualitative comparison

Figure 4a shows the comparison between SCIAMACHY NO_2 VTCs and the corresponding NO_x emission rates for anticyclonic clear sky (pixel cloud fraction ≤0.1) meteorological conditions together with a simple linear regression (n=243). Anticyclonic conditions are deduced from the Alpine Weather Statistics (MeteoSwiss, 1985). Although (i) the present comparison does not include any vertical profile information, (ii)

the smearing effect is not taken into account and (iii) different meteorological conditions can be expected to lead to different relations between the NO_2 VTCs and the corresponding emissions (due to different NO_2/NO ratios and different NO_x lifetimes), the resulting correlation coefficient of R=0.72 indicates that the collocated emissions explain more than 50% of the variance in the NO_2 VTCs. Thus, SCIAMACHY seems to observe the sources of air pollution from space although its sensitivity is strongly decreasing towards the earth's surface.

Figure 4b shows the correlation coefficient vs. the upper limit for the SCIAMACHY cloud fraction; i.e., SCIAMACHY pixels with cloud fractions lower than or equal to this limit have been taken into account. The comparison is carried out for all meteorological conditions as well as for anticyclonic conditions only. We suppose that the better correlations under anticyclonic conditions are due to low wind speeds and rather homogeneous air masses often prevailing during such conditions. Thus, the NO_2 columns are more directly related to the collocated NO_x emissions. Note that the stable values of the correlation coefficients for higher upper cloud fraction limits in Fig. 4b are mainly due to the small number of cases that are additionally taken into account (denoted by the number of data points additionally shown in Fig. 4). The decreasing correlation coefficients with increasing cloud fraction limits can be understood from clouds screening the NO_2 below. In such situations, the retrieved column is strongly affected by the a priori assumption on the vertical NO_2 distribution (Schaub et al., 2006).

4.1.2 Near-ground NO_x lifetime under anticyclonic clear sky conditions

For estimating seasonal NO_x lifetimes we define clear sky conditions to prevail for SCIAMACHY pixels with a cloud fraction ≤ 0.2 (still yielding a correlation coefficient $R > 0.5$ in Fig. 4b). In this way the analysis can be based on a larger data set than available for a limit of 0.1. SCIAMACHY NO_2 VTCs are converted to NO_x VTCs as described in Sect. 3.1.

Figure 5 shows for each season the relationship between individual SCIAMACHY NO_x columns located entirely within the Swiss boundaries and the corresponding NO_x

emission rates between 9:00 and 10:00 UTC. Additionally, the weighted orthogonal regression output is given. The relatively small intercepts suggest that under anticyclonic conditions the background NO_x plays a rather marginal role and the SCIAMACHY observations are dominated by the local NO_x emissions. From the slopes the corresponding column-average NO_x lifetimes for the spring, summer, fall and winter season are calculated as 5.00 ± 0.87, 3.36 ± 0.55, 5.27±0.60 and 11.21±2.13 h, respectively. An additional estimate is calculated using a different time window between 6:00 and 10:00 UTC for summing up the NO_x emission rates. The resulting NO_x lifetimes are summarised in Table 1 and Fig. 6. The alternative time window used to derive the NO_x emission rates (6:00–10:00 UTC instead of 9:00–10:00 UTC) has only a very small impact on the results even though NO_x emission peaks due to morning traffic are included in this case.

Besides the NO_x lifetimes estimated here, Fig. 6 denotes additional summertime lifetime estimates from literature:

- from measurements in power plant plumes: 5 h (Ryerson et al., 1998), 2.8 and 4.2 h (Nunnermacker et al., 2000) and 6.4 h (Sillman, 2000),
- from measurements in urban plumes: Boston: 5.5 h (Spicer, 1982), Nashville: 2.0 h (Nunnermacker et al., 2000), Zurich: 3.2 h (Dommen et al., 1999),
- from GOME NO_2 VTCs above Germany: 6.0 h (Beirle et al., 2003) and
- zonal mean in the boundary layer (0–2 km) from the GEOS-CHEM CTM: 3.0 h (Martin et al., 2003).

For spring, Martin et al. (2003) calculated a mid-latitude NO_x lifetime from the GEOS-CHEM model of 8 h. For the winter season, Martin et al. (2003) and Beirle et al. (2003) reported on NO_x lifetimes of 19 and 21 h, respectively.

Additional NO_x lifetimes are estimated here for the main NO_x loss mechanism which is the oxidation of NO_2 with OH to HNO_3. These estimates are based on typical Swiss

Plateau values of pressure (960 hPa) and temperature and on OH concentrations taken from the BERLIOZ and the SLOPE96 campaigns as well as from long-term OH measurements carried out at Hohenpeissenberg. The BERLIOZ campaign took place at a distance of 50 km from Berlin; the SLOPE96 campaign focused on polluted air masses travelling from the city of Freiburg to the Schauinsland Mountain (south-western Germany); the Hohenpeissenberg station is located in Southern Germany at an altitude of 985 m asl. From a pollution point of view, all regions are similar to the Swiss Plateau and surroundings. For an assumed temperature of 298 K and based on OH concentrations taken from the BERLIOZ and the SLOPE96 campaigns with noontime values of (4–8)$\times 10^6$ cm^{-3} (Volz-Thomas et al., 2003; Mihelcic et al., 2003) and (7–10)$\times 10^6$ cm^{-3} (Volz-Thomas and Kolahgar, 2000), respectively, the resulting mean daytime NO_x lifetimes in summer are estimated to be 4.6 h and 3.0 h. Seasonally averaged 9:00–10:00 UTC OH concentrations determined from clear sky OH measurements at Hohenpeissenberg carried out between 1999 and 2005 (Rohrer and Berresheim, 2006; Berresheim, unpublished data, 2006) are used together with assumed temperatures for the summer, spring/fall and winter seasons of 298 K, 288 K and 278 K, respectively, to estimate NO_x lifetimes of 6.1, 3.9, 8.2 and 21.0 h for the MAM, JJA, SON and DJF seasons, respectively (Fig. 6).

The comparison of our NO_x lifetimes with estimates from literature shows that the summertime values obtained here are reasonable. Our estimate is near the lower end of the range of published values, but it is noteworthy that our values of 3.4 and 3.2 h (depending on the emission time window) perfectly agree with another study carried out in Switzerland by Dommen et al. (1999) yielding a lifetime of 3.2 h (Fig. 6). For spring and fall only few published values are available for comparison (Fig. 6). However, our result is still similar to these values for spring. For the fall season our estimate can only be compared to a lifetime value deduced from Hohenpeissenberg OH measurements and a conclusive statement can not be given. A stronger disagreement is found for winter where our mean NO_x lifetime values are nearly a factor of two smaller than the literature values shown in Fig. 6.

Our wintertime estimate could differ (i) due to the focus on a rather polluted region (in contrast to the zonal mean value given by Martin et al. (2003)), (ii) due to additional wintertime NO_x loss mechanisms besides the oxidation to HNO_3 (which was the only loss considered by Martin et al. (2003) and for calculating the NO_x lifetime from the Hohenpeissenberg OH data) or (iii) due to our approach focusing directly on the location of the NO_x emissions (in contrast to Beirle et al. (2003) who estimated the NO_x lifetime from GOME NO_2 VTCs downwind of emitting regions in Germany). However, based on the fact that the very similar wintertime NO_x lifetime estimates given by Martin et al. (2003) and Beirle et al. (2003) and calculated from the Hohenpeissenberg OH measurements have been derived with independent methods, one could also argue that our wintertime NO_x lifetime estimate (and, possibly, less pronounced also the spring and fall estimates) are too low. The disregard of the horizontal transport (smearing effect) could partly explain our lower values. However, due to the focus on anticyclonic clear sky conditions with enhanced photochemical activity and generally low wind speeds the importance of the smearing effect decreases and we suppose that other reasons could additionally play a role.

In our approach, a higher lifetime is associated with a steeper slope in Fig. 5, i.e. higher space-borne NO_2 VTCs over highly emitting regions. We therefore explore whether, most pronounced in winter, SCIAMACHY retrievals might underestimate the NO_2 VTCs over the polluted Swiss Plateau.

4.2 Comparing GOME and SCIAMACHY NO_2 VTCs over the Swiss Plateau

For a qualitative comparison of clear sky (pixel cloud fraction $\leq$0.1) GOME and SCIAMACHY NO_2 VTCs, the data are mapped onto a fine $0.125^\circ \times 0.125^\circ$ grid covering Switzerland and surroundings. For each cell a mean VTC is computed by averaging over all SCIAMACHY (2003–2005) (Fig. 7a) or GOME (1996–2003) (Fig. 7b) pixels covering the given cell. In contrast to the picture derived from the GOME columns, the higher resolved SCIAMACHY data clearly indicate individual population/industry centres such as the areas of Zurich and Basel as well as the Alpine chain and the Jura

Mountains.

For a more quantitative comparison seasonally averaged GOME and SCIAMACHY NO_2 VTCs are calculated from all clear sky pixels with centre coordinates located within the region ROI_{SP} (Fig. 1) covering the polluted regions of the Swiss Plateau (7° E – 9.5° E, 47° N – 47.75° N) only. Similar to Schaub et al. (2006), the ROI_{SP} excludes the complex Alpine terrain as far as possible. In Fig. 8a the resulting SCIAMACHY NO_2 VTCs are on average higher than the GOME columns in spring, summer and autumn. This can be understood because the extended GOME pixels always include less polluted regions outside of the Swiss Plateau. Surprisingly, the wintertime SCIAMACHY NO_2 VTC values are lower than the ones from GOME.

Figure 8b shows the same comparison with the seasonal mean columns normalised to the spring (MAM) season. Additionally, seasonally averaged NO_2 columns estimated from NO_2 data measured in situ between January 1997 and June 2003 at 15 ground-based sites at different altitudes in Switzerland and Southern Germany are shown. The elevated sites are assumed to detect NO_2 concentrations that are approximately representative for the appropriate height in the (free) troposphere over flat terrain. These measurements, together with boundary layer in situ measurements and an assumed mixing ratio of 0.02 ppb at 8 km, are used to construct NO_2 profiles. The latter are subsequently integrated to tropospheric NO_2 columns. Details on the data set and method of deriving vertical NO_2 profiles/columns can be found in Schaub et al. (2006). For the present study, the ground-based in situ data set is restricted to all clear sky days as indicated by the sunshine and high fog parameters from the Alpine Weather Statistics (MeteoSwiss, 1985) and the columns reach down to an assumed mean Swiss Plateau height of 450 m asl. The normalised seasonal variation of the ground-based data again indicates the highest NO_2 columns over the Swiss Plateau to occur during the winter season, which is better reflected by the GOME columns and expected due to the higher NO_x lifetime in winter. Moreover, the seasonal variation of space-borne NO_2 VTCs over industrialised regions with a distinct wintertime maximum has also been described by Petritoli et al. (2004), Richter et al. (2005), van der A et al. (2006) and Uno et al. (2006).

ACPD
7, 429–468, 2007

EGU

Although in Fig. 8a SCIAMACHY and GOME have been sampled differently in space and time and, thus, a perfect agreement is not expected, it seems likely that SCIAMACHY values over the Swiss Plateau are underestimated in this season. A possible reason for this is discussed in the following section.

4.3 Inaccurate pixel surface pressure as a possible reason for too low wintertime SCIAMACHY NO_2 VTC retrievals over the Swiss Plateau

4.3.1 GOME and SCIAMACHY pixel surface pressures

Richter and Burrows (2002) and Boersma et al. (2004) discussed errors of GOME NO_2 VTC retrievals which in principle also apply to SCIAMACHY retrievals. They reported on the following retrieval parameters inducing inaccuracies in the AMF calculation, which is the major error source for tropospheric retrievals over polluted regions: the a priori NO_2 profile shape, the surface albedo, cloud characteristics (fraction and height) and aerosol concentration. Here, we propose an additional source for systematic errors of SCIAMACHY NO_2 VTCs over the Swiss Plateau: the mean surface pressure (or height) assumed for the retrieval of an individual pixel. This influence has not been investigated in the literature so far. Note that for large parts of the world, the mean surface pressures taken from global models are accurate enough. Over the Alpine topography, however, mean surface pressures taken from a coarsely resolved model could be problematic, particularly for higher resolved satellite pixels. Figure 9 illustrates the situation over the Alpine region: in a coarsely resolved model (e.g. global CTM used for the retrieval), the topography is averaged over extended grid elements, typically leading to an underestimation of the effective elevation of mountains and an overestimation of the effective ground height in the vicinity of the mountains. Due to the different horizontal extensions of GOME and SCIAMACHY pixels, it can be expected that the mean model heights calculated over the smaller SCIAMACHY pixels show a larger deviation from the averaged real surface heights than the mean model heights calculated over the extension of a GOME pixel.

For each GOME (1996–2003) and SCIAMACHY (2003–2005) pixel above ROI_{CH} (Fig. 1) the original mean pixel surface pressure p_{surf} derived from ECMWF/TM4 and p_{eff} determined from the aLMo topography (Sect. 3.2) are converted to m asl based on pressure profiles derived from measurements at different altitudes in Switzerland. Figure 10 shows the resulting histogram distribution of $\Delta surf = h_{surf} - h_{eff}$ for the GOME (Fig. 10a) and SCIAMACHY (Fig. 10b) pixels and Fig. 11 indicates the pixel centre locations and corresponding values of Δsurf. The following conclusions can be drawn:

- Due to the smoothed topography in ECMWF/TM4, the surface heights of the GOME and SCIAMACHY pixels are underestimated over the Alps and overestimated over the Swiss Plateau (Fig. 11).
- Lower minimum and higher maximum for Δsurf are found for SCIAMACHY pixels (Figs. 10 and 11). This can be expected due to the smaller pixel size of SCIAMACHY compared to GOME (Fig. 9).

The above points confirm our expectation that certain parameters, such as the mean pixel surface pressure, can become increasingly inaccurate for better resolved satellite data if the spatial resolution of the forward model parameters is not improved accordingly. In the following section, the effect of an inaccurate pixel surface pressure on the resulting NO_2 VTC is investigated for selected SCIAMACHY columns.

4.3.2 Effect of inaccurate pixel surface pressure on SCIAMACHY retrievals

Figure 12 illustrates the situation over the Swiss Plateau where $h_{surf} > h_{eff}$ (for the Alps the situation is reversed with $h_{surf} < h_{eff}$). Following Eq. (1) (Sect. 2.1) and the formulation for the AMF_{trop} given there, the following systematic errors due to inaccurate surface heights are expected:

- For positive Δsurf ($h_{surf} > h_{eff}$; e.g. over the Swiss Plateau, Figs. 11 and 12) the near-ground NO_2 pollution is in reality located at a lower level than assumed in the

data retrieval. The retrieval therefore associates the high near-ground pollution with a too high sensitivity. This leads to an overestimated AMF_{trop} and, thus, to an underestimated NO_2 VTC.

– For negative Δsurf (h_{surf}<h_{eff}, e.g. over the Alps, Fig. 11) we expect a tendency towards overestimation of the NO_2 VTCs.

The effect of inaccurate pixel surface pressures is investigated following the method described in Sect. 3.2. Clear sky SCIAMACHY NO_2 VTCs are selected over the north-eastern Swiss Plateau with a smooth topography (Fig. 2). Table 2 presents an overview over the SCIAMACHY pixel parameters and the (re-)processed $AMFs_{trop}$. The comparison of the surface pressures p_{surf} and p_{eff} shows that in the region of the north-eastern Swiss Plateau the surface pressures differ by about 50 hPa, which corresponds to ~450 m.

The mean relative change in the $AMFs_{trop}$ due to the changing pixel surface pressure is –27.2±1.3% and –11.7±1.8% for the profile shapes A and B (Fig. 3), respectively. The mean relative change in the resulting NO_2 VTCs is +37.5±2.4% and +13.3±2.4%, respectively. Obviously, the changes in the $AMFs_{trop}$ and the NO_2 VTCs due to changes in the pixel surface pressure are strongly dependent on the NO_2 profile shape. Given the distinctly different shapes A and B, the 13–38% NO_2 VTC error range is a reasonable first estimate of the effect of errors in the pixel surface pressure over a non-trivial topography.

The present sensitivity study is a first-order estimate of the effect of changing pixel surface pressure for a limited subset of SCIAMACHY pixels and based on assumed a priori profile shapes. Depending on the NO_x emissions taking place at the pixel location, photochemical activity and prevailing meteorological conditions, real NO_2 profile shapes can differ from the shapes A and B used here. Nevertheless, we suggest that inaccurate pixel surface pressures used for the NO_2 retrieval over regions with a marked topography can have a considerable effect on the resulting columns. For retrievals in the UV-visible spectral range with a significant decrease of the sensitivity

towards the earth's surface, this effect is of major importance when the NO_2 resides close to the ground. This situation is most pronounced in winter. Thus, the tendency for underestimated wintertime SCIAMACHY NO_2 VTCs over the Swiss Plateau described earlier could at least partly be explained by inaccuracies in the mean pixel surface pressure.

For GOME NO_2 VTCs over heavily polluted regions (NO_2 VTC>1.0×10^{15} molec cm^{-2}), Boersma et al. (2004) estimated mean AMF_{trop} uncertainties of 15%, 2%, 15% and 9% due to inaccuracies in the cloud fraction, the cloud top height, the surface albedo and the a priori NO_2 profile shape, respectively. Even though GOME uncertainties can not directly be transferred to SCIAMACHY retrievals, the orders of magnitude let us assume that the effect of an inaccurate pixel surface pressure on the AMF_{trop} of 12–27% is of equal importance as other types of errors for tropospheric retrievals over regions with a marked topography such as Switzerland.

5 Summary and conclusions

This study has evaluated SCIAMACHY NO_2 VTCs above Switzerland and the Alpine region. The clear relationship between a spatially and temporally highly resolved Swiss NO_x emission inventory and SCIAMACHY NO_2 columns under anticyclonic meteorological conditions has demonstrated the ability of SCIAMACHY to detect the main NO_x pollution features in Switzerland. The decreasing correlation between the two quantities when taking into account cloudy pixels indicates that SCIAMACHY is less likely to accurately detect sources of air pollution in cloudy situations. From the relation between the SCIAMACHY data and the NO_x emission inventory, seasonal NO_x lifetime estimates have been derived. Summertime NO_x lifetimes have been found to be 3.2–3.4 h. These values agree well with lifetime estimates from literature. The plausibility of the NO_x lifetimes estimated for winter is difficult to assess because of the lack of such data in literature. The values found from two studies and calculated here based on

OH concentration data are not necessarily representative for the study region. Nevertheless, an underestimation of the wintertime NO_x lifetime based on the SCIAMACHY measurements can not be ruled out.

A comparison of SCIAMACHY and GOME NO_2 VTCs has shown the improvement of better resolved space-borne data with regard to monitoring the NO_2 pollution distribution on a regional scale. However, the quantitative comparison of seasonally averaged SCIAMACHY and GOME NO_2 VTCs provides evidence for SCIAMACHY NO_2 VTCs tending to systematically underestimate the tropospheric NO_2 columns over the Swiss Plateau during winter. This is further supported by the seasonal variation of NO_2 measured at ground-based in situ sites that is better reflected in the GOME columns.

A possible explanation for underestimated SCIAMACHY NO_2 VTCs over the Swiss Plateau is the use of inaccurate satellite pixel surface pressures derived from coarsely resolved global models in the retrieval. It has been found that the marked topography in the Alpine region can lead to deviations of several hundred meters between the assumed and the real mean surface height over a pixel, particularly pronounced for the smaller sized SCIAMACHY pixels. The resulting effect has been estimated based on selected clear sky SCIAMACHY NO_2 VTCs over the Swiss Plateau and two fixed a priori NO_2 profile shapes. An effect in the 10–40% range has been found for different profile shapes. Although real NO_2 profile shapes can differ from the fixed profiles used for the sensitivity study, the result suggests that inaccurate pixel surface pressures have a considerable effect on the NO_2 column retrieval.

In general, for the air pollution monitoring on a regional scale, higher resolved space-borne data are strongly required and very useful. SCIAMACHY NO_2 VTCs have shown to be sensitive to the near-ground NO_2 pollution in Switzerland. However, we further conclude from this study that in order to fully exploit the potential of such data, the retrieval should be done on a scale that better fits the satellite pixel size. This is of increasing importance with regard to the decreasing pixel sizes from $320\times40\,km^2$ (GOME) to $60\times30\,km^2$ (SCIAMACHY) to $13\times24\,km^2$ (OMI).

Acknowledgements. This work was funded by the Swiss Federal Office for the Environment

(FOEN). For providing information on ground-based NO_2 measurements in Switzerland we acknowledge the Swiss National Air Pollution Monitoring Network (NABEL) and M. Steinbacher. Furthermore we thank I. DeSmedt and M. Van Roozendael (BIRA/IASB) and H. Eskes and R. van der A (KNMI) for their work on making available the TEMIS GOME and SCIAMACHY NO_2 data set used in this study.

References

Beirle, S., Platt, U., Wenig, M., and Wagner, T.: Weekly cycle of NO_2 by GOME measurements: a signature of anthropogenic sources, Atmos. Chem. Phys., 3, 2225–2232, 2003, http://www.atmos-chem-phys.net/3/2225/2003/.

Beirle, S., Platt, U., Wenig, M., and Wagner, T.: Highly resolved global distribution of tropospheric NO_2 using GOME narrow swath mode data, Atmos. Chem. Phys., 4, 1913–1924, 2004, http://www.atmos-chem-phys.net/4/1913/2004/.

Boersma, K. F., Eskes, H. J., and Brinksma, E. J.: Error analysis for tropospheric NO_2 retrieval from space, J. Geophys. Res., 109, art. no. 4311, 2004.

Bovensmann, H., Burrows, J. P., Buchwitz, M., Frerick, J., Noël, S., and Rozanov, V. V.: SCIAMACHY: Mission objectives and measurement modes, J. Atmos. Sci., 56, 2, 127–150, 1999.

Burrows, J. P., Weber, M., Buchwitz, M., Rozanov, V., Ladstätter-Weissenmayer, A., Richter, A., DeBeek, R., Hoogen, R., Bramstedt, K., Eichmann, K. U., Eisinger, M., and Perner, D.: The global ozone monitoring experiment (GOME): Mission concept and first scientific results, J. Atmos. Sci., 56, 151–175, 1999.

Chu, S. H. and Meyer, E. L.: Use of ambient ratios to estimate impact of NO_x sources on annual NO_2 concentrations, Proceedings, 84^{th} Annual Meeting & Exhibition of the Air & Waste Management Association, Vancouver, B.C., 16–21 June 1991, 16 pp., 1991.

Dentener, F. J. and Crutzen, P. J.: Reaction of N_2O_5 on tropospheric aerosols: impact on the global distributions of NO_x, O_3 and OH, J. Geophys. Res., 98, 7149–7163, 1993.

Dentener, F. J., van Weele, M., Krol, M., Houweling, S., and van Velthoven, P.: Trends and inter-annual variability of methane emissions derived from 1979–1993 global CTM simulations, Atmos. Chem. Phys., 3, 73–88, 2003, http://www.atmos-chem-phys.net/3/73/2003/.

Dommen, J., Prévôt, A. S. H., Hering, A. M., Staffelbach, T., Kok, G. L., and Schillawski, R. D.: Photochemical production and aging of an urban air mass, J. Geophys. Res., 104, D5, 5493–5509, 1999.

Eskes, H. J.: Combined retrieval, modeling and assimilation approach to GOME NO_2, in GOA final report, European Commission 5th framework programme 1998–2002, EESD-ENV-99-2, 116–122, Eur. Comm., De Bilt, Netherlands, 2003.

Finlayson-Pitts, B. J. and Pitts, J. N.: Chemistry of the upper and lower Atmosphere - Theory, Experiments and Applications, Academic Press, San Diego, CA, 2000.

FOEN (Swiss Federal Office for the Environment, BAFU): Vom Menschen verursachte Luftschadstoffemissionen in der Schweiz von 1900 bis 2010, Schriftenreihe Umwelt Nr. 256, 1995.

FOEN (Swiss Federal Office for the Environment, BAFU): NABEL – Luftbelastung 2004, Schriftenreihe Umwelt Nr. 388, 2005.

IPCC, Climate Change 2001: The Scientific Basis. Contribution of Working Group I to the Third Assessment Report of the Intergovernmental Panel on Climate Change, Cambridge University Press, Cambridge, UK and New York, USA, 2001.

Jaeglé, L., Jacob, D. J., Wang, Y., Weinheimer, A. J., Ridley, B. A., Campos, T. L., Sachse, G. W., and Hagen, D. E.: Sources and chemistry of NO_x in the upper troposphere over the United States, Geophys. Res. Lett., 25, 1705–1708, 1998.

Keller, J., Andreani-Aksoyoglu, S., Tinguely, M., and Prévôt, A. S. H.: Emission Scenarios 1985–2010: Their Influence on Ozone in Switzerland, PSI Bericht Nr. 05-07, Paul Scherrer Institut, Villigen PSI, 2005.

Keller, M. and Zbinden, R.: Luftschadstoffemissionen des Strassenverkehrs 1980–2030, Schriftenreihe Umwelt Nr. 355, FOEN (Swiss Federal Office for the Environment), 2004.

Koelemeijer, R. B. A., Stammes, P., Hovenier, J. W., and de Haan, J. F.: A fast method for retrieval of cloud parameters using oxygen A-band measurements from Global Ozone Monitoring Experiment, J. Geophys. Res., 106, 3475–3490, 2001.

Kramm, G., Dlugi, R., Dollard, G. J., Foken, T., Mölders, N., Müller, H., Seiler, W., and Sievering, H.: On the dry deposition of ozone and reactive nitrogen species, Atmos. Environ., 29, 3209–3231, 1995.

Kühlwein, J.: Uncertainties in the arithmetical determination of pollutant emissions from road traffic and demands on future models, PhD thesis, University of Stuttgart, 2004.

Kühlwein, J. and Friedrich, R.: Uncertainties of modelling emissions from road transport, At-

mos. Environ., 34, 4603–4610, 2000.
Kunhikrishnan, T., Lawrence, M. G., von Kuhlmann, R., Richter, A., Ladstätter-Weissenmayer, A., and Burrows, J. P.: Analysis of tropospheric NO_x over Asia using the model of atmospheric transport and chemistry (MATCH-MPIC) and GOME-satellite observations, Atmos. Environ., 38, 581–596, 2004.
Leue, C., Wenig, M., Wagner, T., Klimm, O., Platt, U., and Jahne, B.: Quantitative analysis of NO_x emissions from Global Ozone Monitoring Experiment satellite image sequences, J. Geophys. Res., 106, 5493–5505, 2001.
Martin, R. V., Jacob, D. J., Chance, K., Kurosu, T. P., Palmer, P. I., and Evans, M. J.: Global inventory of nitrogen oxide emissions constrained by space-based observations of NO_2columns, J. Geophys. Res., 108, D17, 4537, doi:10.1029/2003JD003453, 2003.
MeteoSwiss: Alpine Weather Statistics (Alpenwetterstatistik - Witterungskalender: Beschreibung der einzelnen Parameter), MeteoSwiss, Switzerland, 1985.
Mihelcic, D., Holland, F., Hofzumahaus, A., Hoppe, L., Konrad, S., Müsgen, P., Pätz, H.-W., Schäfer, H.-J., Schmitz, T., Volz-Thomas, A., Bächmann, K., Schlomski, S., Platt, U., Geyer, A., Alicke, B., and Moortgat, G. K.: Peroxy radicals during BERLIOZ at Pabsttum: measurements, radical budgets and ozone production, J. Geophys. Res., 108, D4, 8254, doi:10.1029/2001JD001014, 2003.
Nakamura, K., Kondo, Y., Chen, G., Crawford, J. H., Takegawa, N., Koike, M., Kita, K., Miyazaki, Y., Shetter, R. E., Lefer, B. L., Avery, M., and Matsumoto, J.: Measurement of NO_2 by the photolysis conversion technique during the Transport and Chemical Evolution Over the Pacific (TRACE-P) campaign, J. Geophys. Res., 108, art. no. 4752, doi:10.1029/2003JD003712, 2003.
Nunnermacker, L. J., Kleinman, L. I., Imre, D., Daum, P. H., Lee, Y.-N., Lee, J. H., Springston, S. R., and Newman, L.: NO_y lifetimes and O_3 production efficiencies in urban and power plant plumes: analysis of field data, J. Geophys. Res., 105, D7, 9165–9176, 2000.
Palmer, P. I., Jacob, D. J., Chance, K., Martin, R. V., Spurr, R. J. D., Kurosu, T. P., Bey, I., Yantosca, R., Fiore, A., and Li, Q.: Air mass factor formulation for spectroscopic measurements from satellites: Application to formaldehyde retrievals from the Global Ozone Monitoring Experiment, J. Geophys. Res., 106, 14 539–14 550, 2001.
Palmer, P. I., Jacob, D. J., Fiore, A. M., Martin, R. V., Chance, K., and Kurosu, T. P.: Mapping isoprene emissions over North America using formaldehyde column observations from space, J. Geophys. Res., 108, D6, 4180, doi:10.1029/2002JD002153, 2003.

Petritoli, A., Bonasoni, P, Giovanelli, G., Ravegnani, F., Kostadinov, I., Bortoli, D., Weiss, A., Schaub, D., Richter, A., and Fortezza, F.: First comparison between ground-based and satellite-borne measurements of tropospheric nitrogen dioxide in the Po basin, J. Geophys. Res., 109, D15307, doi:10.1029/2004JD004547, 2004.

Richter, A. and Burrows, J. P.: Tropospheric NO_2 from GOME measurements, Adv. Space Res., 29, 1673–1683, 2002.

Richter, A., Burrows, J. P., Nüss, H., Granier, C., and Niemeier, U.: Increase in tropospheric nitrogen dioxide over China observed from space, Nature, 437, doi:10.1038/nature04092, 2005.

Rohrer, F. and Berresheim, H.: Strong correlation between levels of tropospheric hydroxyl radicals and solar ultraviolet radiation, Nature, 442, 184–187, 2006.

Ryerson, T. B., Buhr, M. P., Frost, G. J., Goldan, P. D., Holloway, J. S., Hübler, G., Jobson, B. T., Kuster, W. C., McKeen, S. A., Parrish, D. D., Roberts, J. M., Sueper, D. T., Trainer, M., Williams, J., and Fehsenfeld, F. C.: Emissions lifetimes and ozone formation in power plant plumes, J. Geophys. Res., 103, D17, 22 569–22 583, 1998.

Schaub, D., Boersma, K. F., Kaiser, J. W., Weiss, A. K., Eskes, H. J., and Buchmann, B.: Comparison of GOME tropospheric NO_2 columns with NO_2 profiles deduced from ground-based in situ measurements, Atmos. Chem. Phys., 6, 3211–3229, 2006, http://www.atmos-chem-phys.net/6/3211/2006/.

Schaub, D., Weiss, A. K., Kaiser, J. W., Petritoli, A., Richter, A., Buchmann, B., and Burrows, J. P.: A transboundary transport episode of nitrogen dioxide as observed from GOME and its impact in the Alpine region, Atmos. Chem. Phys., 5, 23–37, 2005, http://www.atmos-chem-phys.net/5/23/2005/.

Seinfeld, J. H. and Pandis, S. N.: Atmospheric chemistry and physics - from air pollution to climate change, John Wiley & Sons, New York, 1998.

Sillman, S.: Ozone production efficiency and loss of NO_x in power plant plumes: photochemical model and interpretation of measurements in Tennessee, J. Geophys. Res., 105, D7, 9189–9202, 2000.

Solomon, S., Portmann, W., Sanders, R. W., Daniel, J. S., Madsen, W., Bartram, B., and Dutton, E. G.: On the role of nitrogen dioxide in the absorption of solar radiation, J. Geophys. Res., 104, 12 047–12 058, 1999.

Spicer, C. W.: Nitrogen oxide reactions in the urban plume of Boston, Science, 215, 4536, 1095–1097, 1982.

Stammes, P.: Spectral radiance modelling in the UV-Visible Range, in IRS 2000: Current problems in Atmospheric Radiation, Eds. W. L. Smith and Y. M. Timofeyev, A. Deepak Publ., Hampton (VA), 2001.

Uno, I., He, Y., Ohara, T., Yamaji, K., Kurokawa, J.-I., Katayama, M., Wang, Z., Noguchi, K., Hayashida, S., Richter, A., and Burrows, J. P.: Systematic analysis of interannual and seasonal variations of model-simulated tropospheric NO_2 in Asia and comparison with GOME-satellite data, Atmos. Chem. Phys. Disc., 6, 11 181–11 207, 2006.

Van der A, R. J., Peters, D. H. M. U., Eskes, H., Boersma, K. F., Van Roozendael, M., De Smedt, I., and Kelder, H. M.: Detection of the trend and seasonal variation in tropospheric NO_2 over China, J. Geophys. Res., 111, D12317, doi:10.1029/2005JD006594, 2006.

Vandaele, A. C., Fayt, C., Hendrick, F., et al.: An intercomparison campaign of ground-based UV-visible measurements of NO_2, BrO, and OClO slant columns: Methods of analysis and results for NO_2, J. Geophys. Res., 110, D08305, doi:10.1029/2004JD005423, 2005.

Volz-Thomas, A., Geiss, H., Hofzumahaus, A., and Becker, K.-H.: Introduction to special section: photochemistry experiment in BERLIOZ, J. Geophys. Res., 108, D4, 8252, doi:10.1029/2001JD002029, 2003.

Volz-Thomas, A. and Kolahgar, B: On the budget of hydroxyl radicals at Schauinsland during the Schauinsland Ozone Precursor Experiment (SLOPE96), J. Geophys. Res., 105, D1, 1611–1622, 2000.

Warneck, P.: Chemistry of the natural atmosphere, second edition, Academic Press, London, 2000.

York, D.: Least-square fitting of a straight line, Can. J. Phys., 44, 1079–1086, 1966.

Table 1. Seasonal NO_x lifetime estimates based on a weighted orthogonal regression for two different time windows for averaging the emission rates over the SCIAMACHY pixels. The standard deviations are given by the standard deviations of the slopes of the regression lines.

emission rates (time window)	τ_{NO_x} (hrs) MAM (± std. dev.) n=57	τ_{NO_x} (hrs) JJA (± std. dev.) n=116	τ_{NO_x} (hrs) SON (± std. dev.) n=149	τ_{NO_x} (hrs) DJF (± std. dev.) n=42
9–10 UTC	5.00 (±0.87)	3.36 (±0.55)	5.27 (±0.60)	11.21 (±2.13)
6–10 UTC	4.90 (±0.86)	3.22 (±0.53)	5.23 (±0.59)	11.53 (±2.19)

Table 2. Date, orbit/pixel number, cloud fraction, mean pixel specific ECMWF/TM4 surface pressure p_{surf}, mean pixel specific aLMo surface pressure p_{eff}, AMF_{trop} based on p_{surf} and AMF_{trop} based on p_{eff} for the selected SCIAMACHY pixels. Further denoted are the resulting relative changes in both the $AMFs_{trop}$ and the NO_2 VTCs.

Date	Orbit, pixel number	Cloud fraction	p_{surf} from ECMWF/TM4 [hPa]	p_{eff} from aLMo [hPa]	AMF_{trop} calc. for p_{surf}	AMF_{trop} calc. for p_{eff}	rel. change AMF_{trop} [%]	rel. change NO_2 VTC [%]
Profile A (Fig. 3)								
10 Mar 04	7, 1117	0.024	912.22	964.22	1.023	0.776	–24.1	+ 31.8
22 Jan 05	6, 574	0.011	903.92	956.62	1.315	0.941	–28.4	+ 39.7
22 Jan 05	6, 575	0.033	911.71	963.08	1.359	0.982	–27.7	+ 38.4
17 Nov 05	8, 731	0.008	899.13	948.72	1.326	0.958	–27.8	+ 38.4
17 Nov 05	8, 732	0.011	906.25	958.03	1.308	0.942	–28.0	+ 38.9
17 Nov 05	8, 764	0.009	895.73	950.36	1.315	0.944	–28.2	+ 39.3
23 Nov 05	7, 493	0.074	919.30	970.80	1.241	0.904	–27.2	+ 37.3
23 Nov 05	7, 559	0.000	912.22	958.68	1.257	0.916	–27.1	+ 37.2
26 Nov 05	7, 701	0.058	884.32	941.34	1.215	0.890	–26.7	+ 36.5
Profile B (Fig. 3)								
17 Apr 04	5, 1383	0.012	899.71	953.97	1.109	0.972	–12.4	+ 14.1
12 May 04	7, 726	0.019	903.72	955.69	1.106	0.933	–15.6	+ 18.5
21 Jul 04	8, 674	0.005	913.20	963.67	1.004	0.889	–11.5	+ 12.9
21 Jul 04	8, 691	0.027	916.65	963.47	0.963	0.858	–10.9	+ 12.2
09 Aug 04	8, 645	0.014	905.58	959.25	0.936	0.835	–10.7	+ 12.1
03 Jul 05	8, 645	0.092	912.73	962.94	0.897	0.803	–10.5	+ 11.7
10 Aug 05	8, 614	0.006	905.79	962.17	0.895	0.801	–10.5	+ 11.7

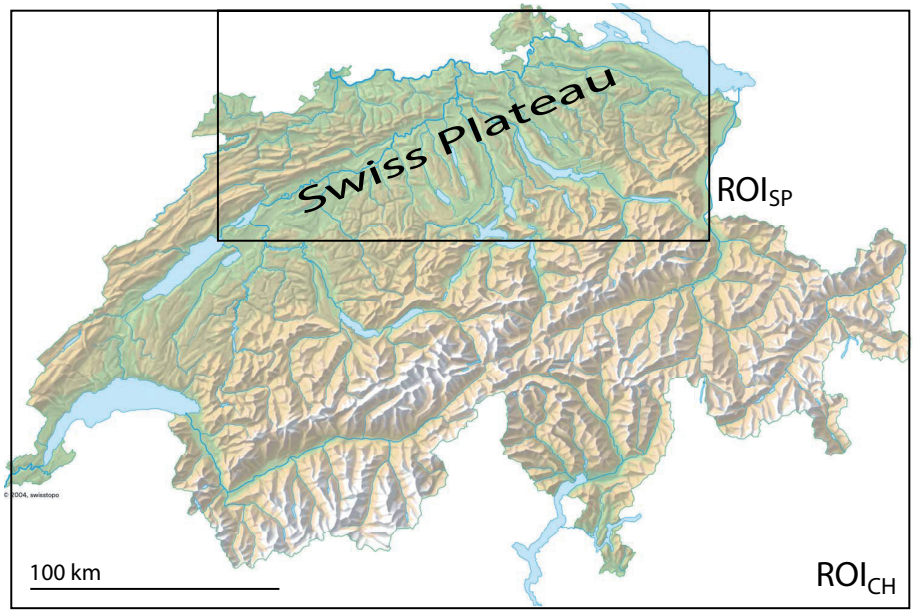

Fig. 1. Regions of interest used in this study covering the whole Switzerland (6° E–10.5° E, 45.75° N–47.75° N, ROI$_{CH}$) and the polluted Swiss Plateau (7° E–9.5° E, 47° N–47.75° N, ROI$_{SP}$). (Topographic map of Switzerland: © 2005 swisstopo).

ACPD
7, 429–468, 2007

EGU

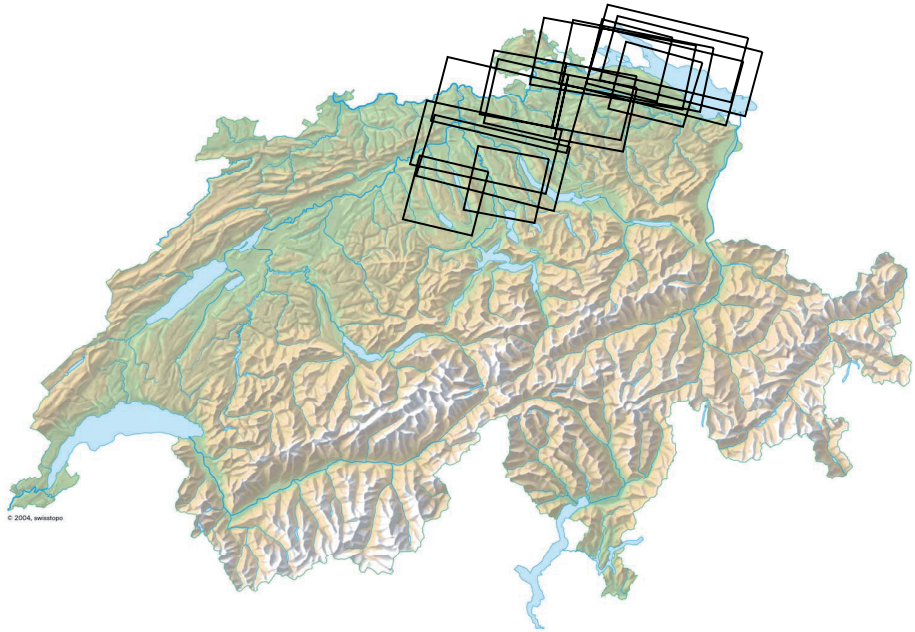

Fig. 2. Topographic map of Switzerland (© 2005 swisstopo) with the location of the SCIAMACHY pixels used for the pixel surface pressure sensitivity calculation.

ACPD

7, 429–468, 2007

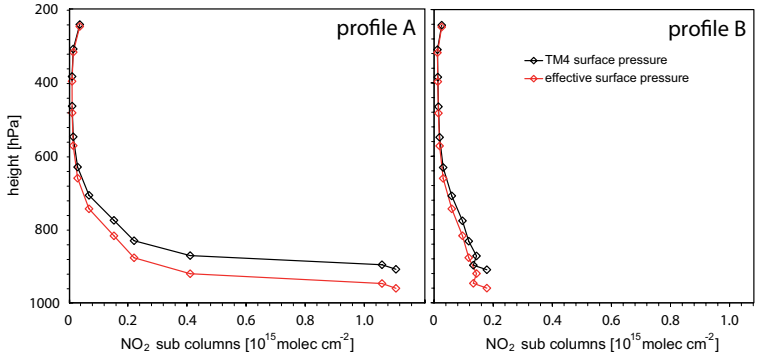

Fig. 3. CTM a priori NO_2 profiles A (poor vertical mixing/polluted) and B (strong vertical mixing/remote) given as layer-specific sub columns. The black profiles are associated with the ECMWF/TM4 surface pressure at the location of the SCIAMACHY pixel. The red profiles are reaching down to the effective surface pressure calculated from the aLMo model with a $7 \times 7\,km^2$ resolution. For the examples shown here, surface pressures are taken from 10 March 2004 (profile A) and from 21 July 2001 (profile B).

ACPD
7, 429–468, 2007

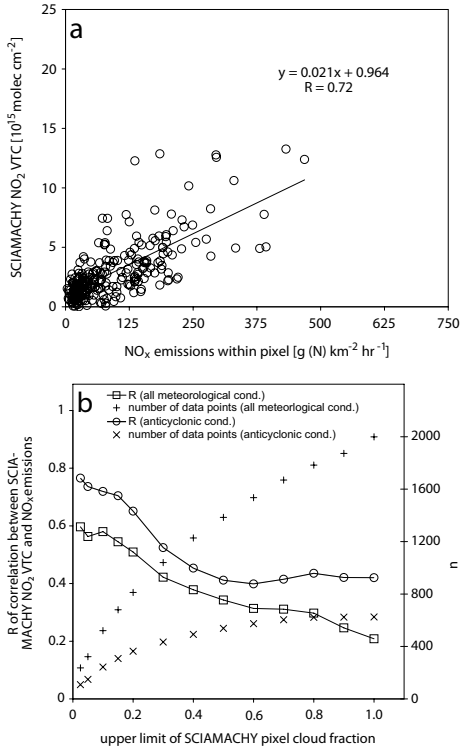

Fig. 4. Comparison between SCIAMACHY NO_2 VTCs (from 2003–2005) and collocated NO_x emission rates for pixels located entirely within the Swiss boundaries and anticyclonic clear sky meteorological conditions (pixel cloud fraction ≤ 0.1, n=243) **(a)**. Correlation coefficients of the present comparison for different upper limits of cloud fraction **(b)**.

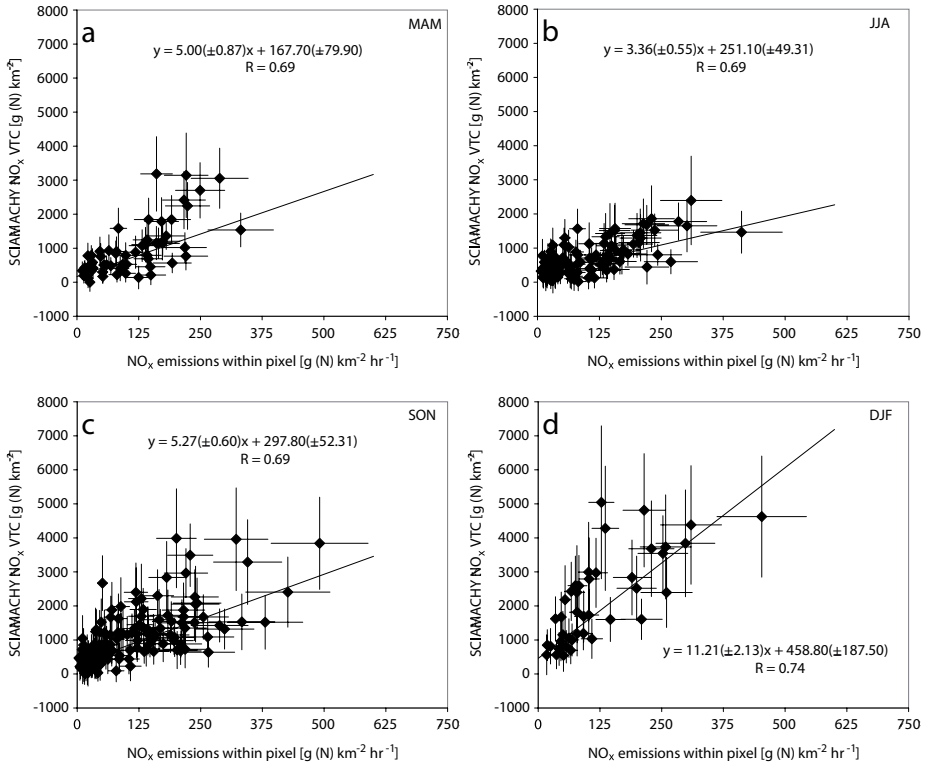

Fig. 5. Clear sky (cloud fraction ≤ 0.2) SCIAMACHY NO_x VTCs located entirely within the Swiss boundaries vs. NO_x emission rates (both given in N-equivalents). NO_2 VTCs are converted to NO_x VTCs using assumed values for the seasonal mean NO_2/NO ratios. The resulting NO_x VTCs are compared to NO_x emission rates enclosed within the individual pixels for the four seasons spring **(a)**, summer **(b)**, fall **(c)** and winter **(d)**. The examples shown here are based on NO_x emission rates taking place between 9:00 and 10:00 UTC. Additionally, the orthogonal regression calculation output (based on data errors as described in Sect. 3.1) is given (see also Table 1).

ACPD
7, 429–468, 2007

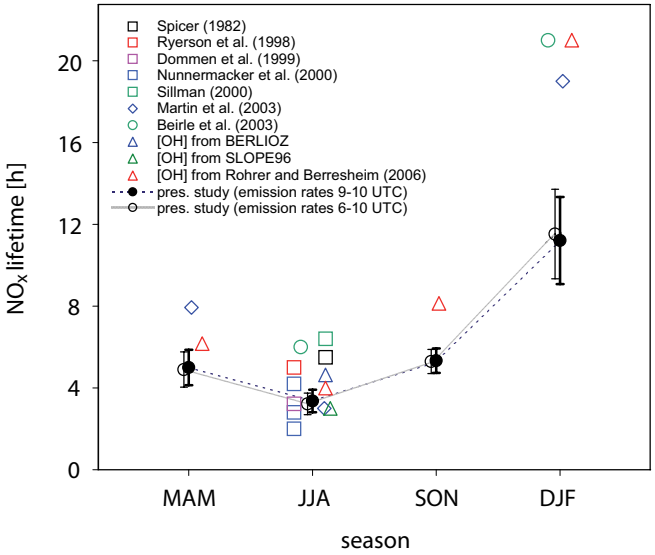

Fig. 6. Seasonal NO_x lifetimes (and standard deviations) over the Swiss Plateau under anticyclonic clear sky conditions estimated in this study. Results from other studies are shown for comparison. These data have been deduced from campaigns in the U.S. (Spicer, 1982; Ryerson et al., 1998; Nunnermacker et al., 2000; Sillman, 2000) and in the Swiss Plateau (Dommen et al., 1999), from GOME NO_2 VTCs over Germany (Beirle et al., 2003) and from the GEOS-CHEM model (Martin et al., 2003). Additionally, mean NO_x lifetimes against oxidation to HNO_3 are calculated for (i) 960 hPa and 298 K with OH concentrations of $(4–8)\times10^6$ cm^{-3} measured during the BERLIOZ campaign (Volz-Thomas et al., 2003; Mihelcic et al., 2003) and of $(7–10)\times10^6$ cm^{-3} measured during the SLOPE96 campaign (Volz-Thomas and Kolahgar, 2000) as well as for (ii) seasonally averaged OH concentrations measured by Rohrer and Berresheim (2006) with 960 hPa and assumed temperatures for the summer, spring/fall and winter seasons of 298 K, 288 K and 278 K, respectively.

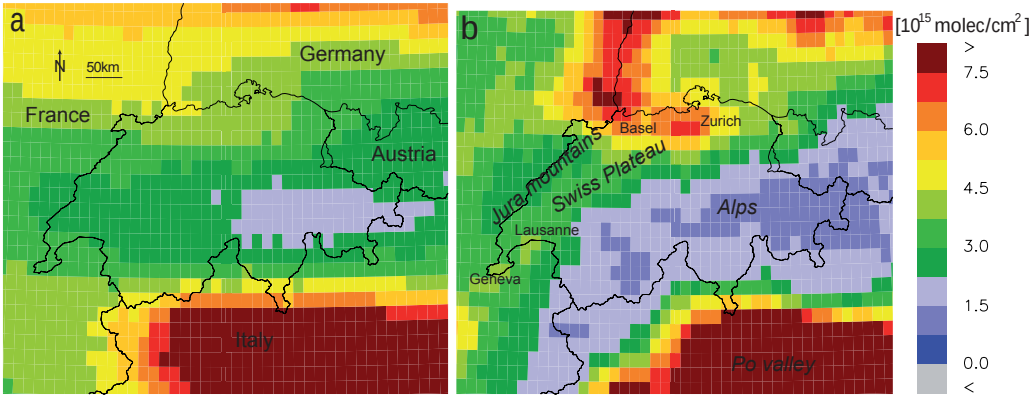

Fig. 7. Mean clear sky (satellite pixel cloud fraction ≤ 0.1) NO_2 tropospheric columns over the Central Alps and Switzerland deduced from GOME (1996–2003) **(a)** and SCIAMACHY (2003–2005) **(b)** retrievals. In contrast to the GOME picture, specific features such as the Alpine chain, the Jura Mountains, the Swiss Plateau and the areas of Greater Zurich and Basel clearly show up in the SCIAMACHY data.

ACPD
7, 429–468, 2007

EGU

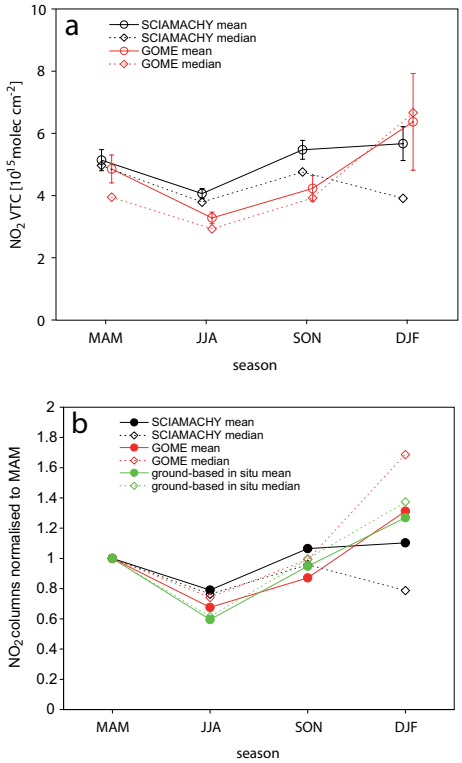

Fig. 8. Seasonal mean and median NO_2 VTCs from GOME and SCIAMACHY over the ROI_{SP} (Fig. 1) for clear sky conditions (cloud fraction ≤ 0.1). For the four seasons MAM, JJA, SON and DJF, SCIAMACHY and GOME contributed with 76, 175, 129 and 86 and 52, 95, 33 and 7 NO_2 VTCs, respectively **(a)**. Seasonal mean and median NO_2 columns from GOME, SCIAMACHY and derived from ground-based in situ NO_2 measurements normalised to the spring (MAM) season. The ground-based in situ columns were calculated following the method and data set described in Schaub et al. (2006) and for a Swiss Plateau ground height of 450 m asl. For the four seasons MAM, JJA, SON and DJF, 139, 165, 69 and 78 columns contribute to the seasonal values **(b)**.

ACPD
7, 429–468, 2007

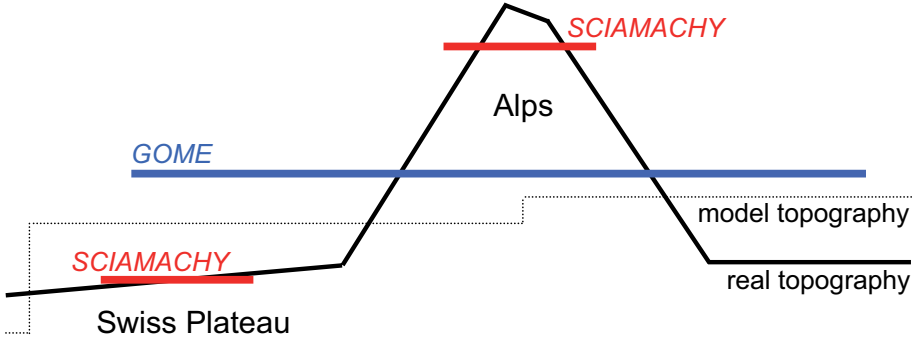

Fig. 9. A simplified illustration of the problem arising for highly resolved satellite pixels over a marked topography when retrieved with coarsely resolved input parameters. The red and blue lines denote the averaged real surface height at the location of individual SCIAMACHY and GOME pixels, respectively. Further, the real topography and the topography given in a coarsely resolved global model are indicated. Over the large GOME pixel extension, the mean height given by a coarsely resolved model better approximates the averaged real surface height than for the smaller SCIAMACHY pixels.

ACPD
7, 429–468, 2007

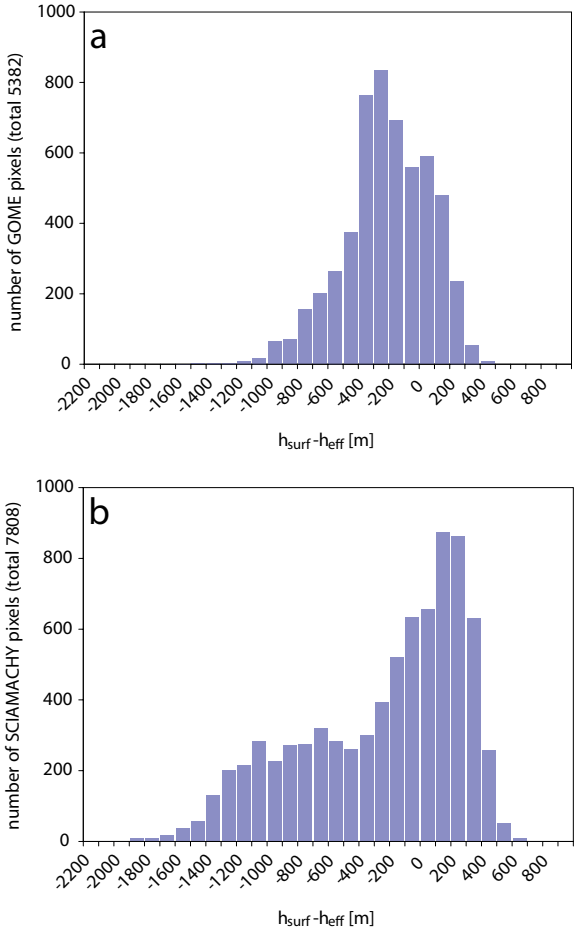

Fig. 10. Histogram distribution of the differences between pixel surface heights used in the retrieval and effective surface heights averaged over the pixels (Δsurf) for all GOME (1996–2003) **(a)** and SCIAMACHY (2003–2005) **(b)** pixels with centre coordinates above ROI_{CH} (Fig. 1).

ACPD
7, 429–468, 2007

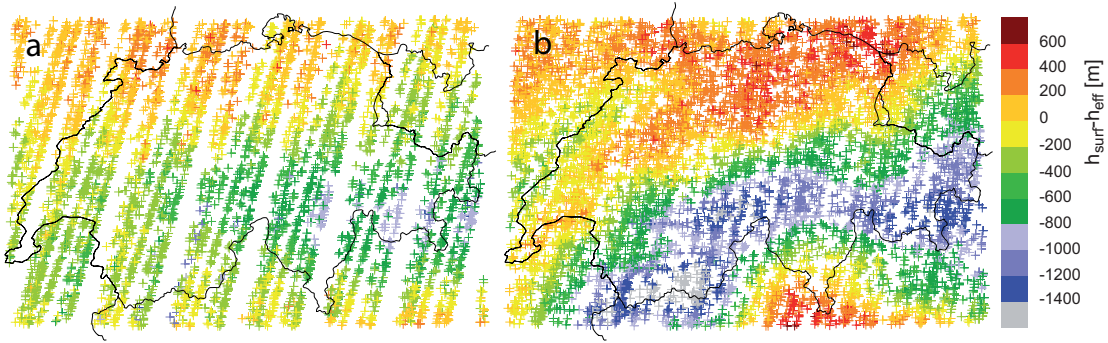

Fig. 11. Differences between pixel surface heights used in the retrieval and effective surface heights averaged over the respective pixels (Δsurf) for all GOME (1996–2003) **(a)** and SCIAMACHY (2003–2005) **(b)** pixels located over ROI_{CH} (Fig. 1). The Δsurf value for a pixel is indicated at its corresponding centre coordinate.

ACPD
7, 429–468, 2007

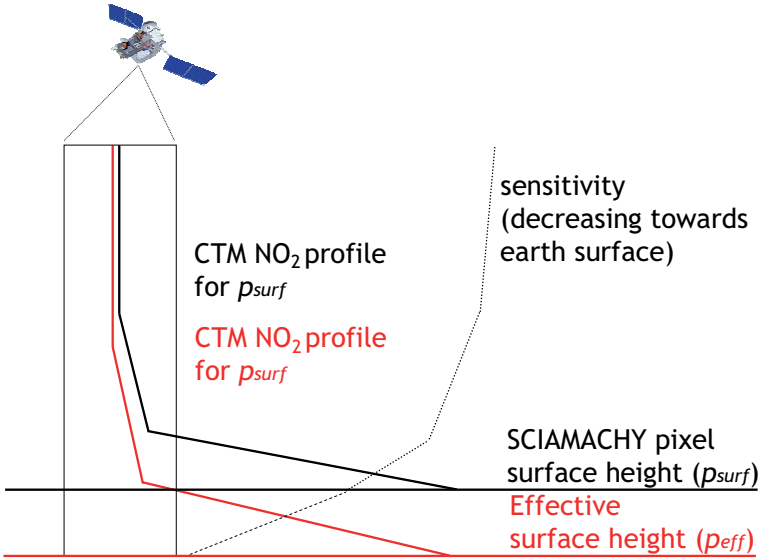

Fig. 12. Possible reason for too low SCIAMACHY NO_2 VTCs over the polluted Swiss Plateau: retrieval errors due to inaccurate pixel surface heights in regions with a marked topography.

ACPD
7, 429–468, 2007